Theta Conditions in Binary and Multicomponent Polymer Solutions Using a Perturbed Hard-Sphere-Chain Equation of State

Stephen M. Lambert, Yuhua Song, and John M. Prausnitz*

Department of Chemical Engineering, University of California, and Chemical Sciences Division, Lawrence Berkeley Laboratory, University of California, Berkeley, California 94720

Received December 14, 1994; Revised Manuscript Received April 20, 1995[®]

ABSTRACT: Theta (Θ) conditions in binary and multicomponent polymer solutions are calculated using a perturbed hard-sphere-chain (PHSC) equation of state. Θ conditions are identified by roots of the spinodal criterion in the limit of infinite polymer molecular weight and zero polymer-segment fraction. Because the thermodynamic properties of mixtures are described by an equation of state, both upper and lower Θ temperatures can be calculated. For binary systems (one polymer and one solvent), experimentally determined Θ conditions and the critical solution temperature for a single polymer molecular weight are used to obtain equation-of-state parameters. Parameters obtained in this manner yield nearly quantitative representation of upper and lower Θ temperatures as a function of pressure and upper and lower critical solution temperatures as a function of polymer molecular weight. For ternary systems (two solvents and one polymer), the dependence of the Θ temperature on solvent composition can be described using parameters obtained from binary data.

1. Introduction

Solvent quality, an important quantity characterizing the behavior of a polymer in solution, is often defined with respect to theta (Θ) conditions. A polymer dissolved in a "better than Θ" i.e., a "good" solvent, is stable and will not phase separate at all concentrations and polymer molecular weights. On the other hand, a polymer dissolved in "worse than Θ", i.e., a "poor" solvent, *may* phase separate at some concentration or polymer molecular weight.[1] In addition to miscibility, the conformational structure of a polymer molecule in dilute solution can also be related to Θ conditions. In a good solvent, an isolated polymer coil is expanded, whereas in a poor solvent, the polymer collapses into a globular structure. At the Θ condition, repulsive excluded-volume interactions exactly counter attractive dispersion forces between polymer segments and the polymer behaves as an ideal chain.[2,3] Also, the behavior of complex systems can sometimes be linked to Θ conditions; for example, the flocculation conditions of sterically stabilized colloidal dispersions correlate strongly with the Θ conditions of the stabilizing polymer moiety.[4] Because Θ conditions characterize both the phase behavior and conformational behavior of polymers in solution, an array of experimental techniques is available for their determination; a few techniques are summarized below.

For a binary mixture of a polymer in a single solvent, the "Shultz–Flory" method is based on a relation between the critical solution temperature and polymer molecular weight; this relation is derived from the Flory–Huggins incompressible-lattice model:[1,5]

$$\frac{1}{T_{\mathrm{CST}}} = \frac{1}{\Theta}\left[1 + \frac{1}{\psi_1}\left(\frac{1}{\sqrt{r}} + \frac{1}{2r}\right)^n\right] \qquad (1)$$

In eq 1, T_{CST} is the critical solution temperature, Θ is the Θ temperature, ψ_1 is the Flory residual-entropy parameter, and r is the ratio of the molecular volume of the polymer to that of the solvent; r is proportional to the polymer molecular weight. For a reliable estimation of the Θ temperature, the Shultz–Flory method requires three or more monodisperse polymer samples of different molecular weight. For each molecular weight, cloud-point temperatures are measured for several solutions spanning a range of polymer segment fractions of approximately 10^{-3}–10^{-1}. If cloud points appear upon decreasing temperature, the minimum temperature as a function of polymer concentration is the lower critical solution temperature (LCST). The reciprocals of the critical solution temperatures are plotted vs $r^{-1/2} + (2r)^{-1}$. Extrapolation to infinite polymer molecular weight (i.e., $r^{-1/2} + (2r)^{-1} = 0$) gives the reciprocal of the Θ temperature.

Since there are two types of critical solution temperatures, two types of Θ temperatures can exist, one associated with the UCST and the other associated with the LCST. Although the Flory–Huggins model can predict only a UCST because it assumes the mixture is incompressible, eq 1 has also been used to correlate the molecular weight dependence of LCSTs. In the original form of eq 1, the exponent n is unity; however, Shultz–Flory plots for some systems can exhibit distinct curvatures. In that event, the *ad hoc* exponent n is adjusted empirically to linearize experimental data to perform a reliable extrapolation to infinite polymer molecular weight.[6–8]

The Flory–Huggins model also shows that the polymer segment fraction at the critical consolute point, $\phi_{\mathrm{polymer}}^{\mathrm{CST}}$, asymptotically approaches zero in the limit of infinite polymer molecular weight:

$$\phi_{\mathrm{polymer}}^{\mathrm{CST}} = \frac{1}{1 + r^{1/2}} \qquad (2)$$

This behavior is observed experimentally, even though the segment fraction at the critical consolute point is difficult to determine accurately from measured cloud-point curves. The behavior of $\phi_{\mathrm{polymer}}^{\mathrm{CST}}$ in the limit of infinite polymer molecular weight plays an important role in devising appropriate criteria which allow the

---

* To whom correspondence should be addressed.

[®] Abstract published in *Advance ACS Abstracts,* June 1, 1995.

0024-9297/95/2228-4866$09.00/0

calculation of Θ conditions from an equation of state for chainlike fluid mixtures.

Another method for experimental determination of Θ conditions is the cloud-point titration method[9-14] and also has theoretical justification from the Flory–Huggins model.[4,15] The cloud-point titration method uses the same type of measurements as the Shultz–Flory method (i.e., turbidimetry), but there are several key differences. First, the cloud-point titration method requires only one molecular weight polymer sample. Second, smaller polymer concentrations are required, typically in the range of 10^{-5}–10^{-2}. The behavior of cloud-point temperatures in this concentration range is summarized by

$$\frac{1}{T_{\mathrm{CP}}} = \frac{1}{\Theta} - B_{\mathrm{T}} \ln \phi_{\mathrm{polymer}} \tag{3}$$

where T_{CP} is the cloud-point temperature and B_{T} is the slope of the cloud-point curve when T_{CP}^{-1} is plotted against ln ϕ_{polymer}. According to eq 3, extrapolation of a plot of the inverse cloud-point temperature vs the logarithm of the polymer concentration to pure polymer ($\phi_{\mathrm{polymer}} = 1$) gives the reciprocal of the Θ temperature. The cloud-point method and the Shultz–Flory method have been shown to produce consistent Θ temperatures for several systems to within experimental uncertainty.[11]

A third difference between these two methods is that the cloud-point titration method can be extended to describe a polymer in a mixed solvent. In this case, a nonsolvent (component 2) is added to a mixture of good-solvent (component 1) and polymer (component 3) at constant temperature until a cloud point is observed. The mixed-solvent composition at the cloud point (ϕ_2^{CP}) is measured for several dilute polymer concentrations, again in the range of $10^{-5} < \phi_3 < 10^{-2}$. The behavior is summarized in a manner similar to eq 3:

$$\phi_2^{\mathrm{CP}} = \phi_2^{\Theta} - B_{\phi} \ln \phi_3 \tag{4}$$

where B_ϕ is the slope of the cloud-point concentration curve when ϕ_2^{CP} is plotted against ln ϕ_3. Extrapolation of ϕ_2^{CP} to pure polymer ($\phi_3 = 1$) gives the "Θ-composition" ϕ_2^{Θ}. Performing titrations at different temperatures gives the dependence of ϕ_2^{Θ} on temperature, or identically, the dependence of Θ on solvent composition.

A third method probes the behavior of another thermodynamic property of dilute polymer solutions: the osmotic second virial coefficient, A_2. Two common experimental techniques for measuring the second osmotic virial coefficient are osmometry[1] and low-angle laser-light scattering.[16] Like the cloud-point titration method, measurement of A_2 requires only a single polymer molecular weight. Θ conditions are determined by scanning temperatures or solvent compositions to find the conditions where the measured value of A_2 is zero.

Additional methods for determining Θ conditions examine the molecular weight dependence of various hydrodynamic properties of polymer solutions. These methods can be generalized by:[1,17]

$$P = KM^a \tag{5}$$

where P is a measured property such as the intrinsic viscosity, sedimentation coefficient, or diffusion coefficient, M is the polymer molecular weight, and K is a proportionality constant. The temperature or solvent composition where the exponent $a = {}^1/_2$ identifies a Θ condition. Like the Shultz–Flory method, this method requires experimental measurements using several molecular weights of a given polymer.

The techniques discussed above probe distinctly different properties (thermodynamic or hydrodynamic) over a wide range of concentration (concentrated vs dilute). Different experimental methods raise questions concerning consistency. Surveying a compiled list of measured Θ conditions for a wide range of polymers, solvents, and experimental techniques[17] is inconclusive. In many cases consistent results are obtained across techniques, but for some systems, results from different methods can differ significantly.

Theoretically, this concern is less ambiguous. Models that describe dilute polymer solutions are fundamentally different from those that describe concentrated polymer solutions (such as the Flory–Huggins model or hard-sphere-chain models). In dilute solutions, the nonuniform distribution of polymer segments is important; however, in concentrated solutions, the spatial distribution of segments is properly assumed to be uniform. As discussed by Flory (ref 1, p 532), this distinction between models becomes unimportant at the Θ condition.

Recently, computer simulations have been performed that probed both phase equilibria and conformational properties of polymers whose segments interact through the Lennard-Jones potential.[18] Simulations which determined phase equilibria were used to construct a Shultz–Flory plot for Lennard-Jones chains. Additional simulations which sampled conformational properties were performed to calculate the second virial coefficient. Although simulated polymer chain lengths were somewhat small, the Θ temperature obtained from the Shultz–Flory plot was found to be near the "Boyle" temperature of large-chain-length polymers. Hard-sphere-chain-based equations of state for pure fluids, such as the PHSC[19] and SAFT[20] equations of state, are based on a similar model of chain structure but neglect long-range correlations. Because of the mean-field nature of these equations of state, direct comparison with computer-simulation results is not meaningful; most likely, the equation-of-state theories produce coexistence curves which are too parabolic in the critical region and overshoot the critical temperature. However, the equations of state should give similar scaling of the critical temperature with polymer chain length.

This paper has three objectives. First, we present a method for calculating Θ conditions using an equation of state for chainlike fluid mixtures. Second, we use experimentally determined Θ conditions (and a minimum amount of additional experimental information) for binary systems to extract equation-of-state parameters that yield quantitative representation of upper and lower critical solution temperatures as a function of pressure and polymer molecular weight. Finally, we attempt to represent quantitatively the Θ temperature of polymers in a mixed solvent using parameters obtained from binary data.

Although the method presented here for the calculation of Θ conditions can be used with any equation of state for chainlike fluids, we perform calculations using the perturbed hard-sphere-chain (PHSC) equation of state.[19,21,22] Other equations of state which could be used include those derived from lattice-fluid models[23-26] and the statistical associated-fluid theory (SAFT).[20,27]

Table 1. Constants Used in Equations 9 and 10

eq 9		eq 10	
α_1	1.8681	β_1	0.7303
α_2	0.0619	β_2	0.1649
α_3	0.6715	β_3	2.3973
α_4	1.7317		

We begin by summarizing the pertinent thermodynamic functions associated with the PHSC equation of state.

2. Equation of State and Thermodynamic Functions

The perturbed hard-sphere-chain (PHSC) equation of state[22] for an m-component mixture is:

$$\frac{p}{\varrho_r k_B T} = 1 + \varrho_r \sum_{ij}^{m} \phi_i \phi_j b_{ij} g_{ij}(\mathrm{d}_{ij}^{+}) - \sum_{i}^{m} \phi_i \left(1 - \frac{1}{r_i}\right) g_{ii}(d_{ii}^{+}) - \frac{\varrho_r}{k_B T} \sum_{ij}^{m} \phi_i \phi_j a_{ij} \quad (6)$$

where p is the pressure, $\varrho_r = N_r/V$ is the segment density ($N_r = \sum_{i=1}^{m} N_i r_i$ is the total number of segments in volume V), $\phi_i = N_i r_i/N_r$ is the segment fraction of component i, k_B is the Boltzmann constant, and T is the absolute temperature. In eq 6, $g_{ij}(d_{ij}^{+})$ is the ij pair radial distribution function of hard-sphere mixtures at contact, b_{ij} is the second virial coefficient of effective hard-sphere mixtures, and a_{ij} reflects the strength of attractive forces between unbonded segments of component i and component j.

According to perturbed hard-sphere-chain theory,[19,22] parameters a_{ii} and b_{ii} are functions of temperature:

$$a_{ii}(T) = \frac{2\pi}{3} \sigma_{ii}^{3} \epsilon_{ii} \mathcal{F}_a(k_B T/\epsilon_{ii}) \quad (7)$$

$$b_{ii}(T) = \frac{2\pi}{3} d_{ii}^{3}(T) = \frac{2\pi}{3} \sigma_{ii}^{3} \mathcal{F}_b(k_B T/\epsilon_{ii}) \quad (8)$$

where d_{ii} is the effective hard-sphere diameter of a segment of component i at temperature T and constants ϵ_{ii} and σ_{ii} characterize the intermolecular potential between unbonded segments of component i; ϵ_{ii} is the depth of the minimum in the pair potential, and σ_{ii} is the separation distance between segment centers at this minimum. For brevity, ϵ_{ii} is referred to as an effective "interaction energy" between nonbonded segments of component i and σ_{ii} is referred to as an effective "hard-core" segment diameter of component i. Functions $\mathcal{F}_a$ and $\mathcal{F}_b$ in eqs 7 and 8 are determined from the thermodynamic properties of simple fluids ($r = 1$) and represented by

$$\mathcal{F}_a(k_B T/\epsilon_{ij}) = \alpha_1 \exp[-\alpha_2 (k_B T/\epsilon_{ij})] + \alpha_3 \exp[-\alpha_4 (k_B T/\epsilon_{ij})^{3/2}] \quad (9)$$

$$\mathcal{F}_b(k_B T/\epsilon_{ii}) = \beta_1 \exp[-\beta_2 (k_B T/\epsilon_{ii})^{1/2}] + (1 - \beta_1) \exp[-\beta_3 (k_B T/\epsilon_{ii})^{3/2}] \quad (10)$$

Constants α_i and β_i are listed in Table 1 and are the same for all fluids. [A simplified version of the PHSC equation is used here. In previous publications, the temperature dependence of the universal functions were scaled by a parameter s which was a function of chain length, r. In the present model, this scale factor is removed and the universal functions were determined from the thermodynamic properties of argon and methane over a wider temperature range. Removal of $s(r)$ from the universal functions allows use of simpler combining rules. The simpler rules do not sacrifice accuracy in fitting thermodynamic properties of pure (nonassociating) fluids to obtain equation-of-state parameters.]

For each pair of components in the mixture, cross terms a_{ij} and b_{ij} are needed. A simple extension of eq 7 is used for a_{ij}:

$$a_{ij}(T) = \frac{2\pi}{3} \sigma_{ij}^{3} \epsilon_{ij} \mathcal{F}_a(k_B T/\epsilon_{ij}) \quad (11)$$

Equation 11 requires combining rules to determine ϵ_{ij} and σ_{ij}:

$$\epsilon_{ij} = (\epsilon_{ii} \epsilon_{jj})^{1/2} (1 - \kappa_{ij}) \quad (12)$$

$$\sigma_{ij} = (\sigma_{ii} + \sigma_{jj})/2 \quad (13)$$

Equation 12 introduces binary interaction parameter κ_{ij}. Unlike a_{ij}, b_{ij} is not arbitrary but is uniquely determined from additivity of effective hard-sphere diameters:

$$b_{ij}(T) = \frac{2\pi}{3} d_{ij}^{3}(T) = \frac{1}{8} (b_{ii}^{1/3} + b_{jj}^{1/3})^{3}; \quad d_{ij}(T) = \frac{1}{2} [d_{ii}(T) + d_{jj}(T)] \quad (14)$$

Finally, the PHSC EOS for mixtures uses for $g_{ij}(d_{ij}^{+})$ the Boublik–Mansoori extension of the Carnahan–Starling equation to mixtures of hard spheres:[28,29]

$$g_{ij}(d_{ij}^{+}) = g_{ij}(\eta, \xi_{ij}) = \frac{1}{1 - \eta} + \frac{3}{2} \frac{\xi_{ij}}{(1 - \eta)^2} + \frac{1}{2} \frac{\xi_{ij}^{2}}{(1 - \eta)^3} \quad (15)$$

where η and ξ_{ij} are packing fractions defined as

$$\eta = \frac{\varrho_r}{4} \sum_{i=1}^{m} \phi_i b_{ii} \quad (16)$$

$$\xi_{ij} = \left(\frac{b_{ii} b_{jj}}{b_{ij}}\right)^{1/3} \frac{\varrho_r}{4} \sum_{k=l}^{m} \phi_k b_{kk}^{2/3} \quad (17)$$

From the equation of state (eq 6), other relevant thermodynamic functions such as the Helmholtz energy and chemical potential are derived using appropriate thermodynamic identities.[30] The Helmholtz energy of the mixture is

$$\frac{A}{N_r k_B T} = \sum_{i=1}^{m} \phi_i \frac{A_i^{\circ}}{N_i r_i k_B T} + \varrho \sum_{i,j=1}^{m} \phi_i \phi_j b_{ij} W_{ij} - \sum_{i=1}^{m} \phi_i \left(1 - \frac{1}{r_i}\right) Q_{ii} - \frac{\varrho_r}{k_B T} \sum_{i,j=1}^{m} \phi_i \phi_j a_{ij} + \sum_{i=1}^{m} \frac{\phi_i}{r_i} \ln\left(\frac{\phi_i}{r_i} \varrho_r k_B T\right) \quad (18)$$

where A_i° is the Helmholtz energy of pure component i

as an ideal gas at temperature T. W_{ij} and Q_{ii} are given by:

$$W_{ij}(\eta,\xi_{ij}) = K_1 + \frac{3}{2}\xi_{ij}K_2 + \frac{1}{2}\xi_{ij}^{\ 2}K_3 \tag{19}$$

$$Q_{ii}(\eta,\xi_{ii}) = -\ln(1-\eta) + \frac{3}{2}\frac{\xi_{ii}}{1-\eta} + \frac{1}{4}\frac{\xi_{ii}^{\ 2}}{(1-\eta)^2} \tag{20}$$

$$K_n = \frac{1}{\eta}\left[-K_{n-1} + \frac{1}{n-1}\frac{1}{(1-\eta)^{n-1}}\right], \qquad K_1 = -\frac{\ln(1-\eta)}{\eta} \tag{21}$$

The chemical potential of component k is

$$\frac{\mu_k}{k_BT} = \frac{\mu_k^{\ \circ}}{k_BT} + 2r_k\varrho_r\sum_{i=1}^{m}\phi_ib_{ik}W_{ik} + \varrho_r\sum_{i,j=1}^{m}\phi_i\phi_jb_{ij}\left(N_r\frac{\partial W_{ij}}{\partial N_k}\right) - (r_k-1)Q_{kk} - \sum_{i=1}^{m}\phi_i\left(1-\frac{1}{r_i}\right)\left(N_r\frac{\partial Q_{ii}}{\partial N_k}\right) - \frac{2r_k\varrho_r}{k_BT}\sum_{i=1}^{m}\phi_ia_{ik} + \ln\left(\frac{\phi_k}{r_k}\varrho_rk_BT\right) + 1 \tag{22}$$

where μ_k° is the chemical potential of pure component i as an ideal gas at temperature T and

$$\left(N_r\frac{\partial W_{ij}}{\partial N_k}\right) = \left(\frac{\partial W_{ij}}{\partial\eta}\right)\left(N_r\frac{\partial\eta}{\partial N_k}\right) + \left(\frac{\partial W_{ij}}{\partial\xi_{ij}}\right)\left(N_r\frac{\partial\xi_{ij}}{\partial N_k}\right) \tag{23}$$

$$\left(N_r\frac{\partial Q_{ii}}{\partial N_k}\right) = \left(\frac{\partial Q_{ii}}{\partial\eta}\right)\left(N_r\frac{\partial\eta}{\partial N_k}\right) + \left(\frac{\partial Q_{ii}}{\partial\xi_{ii}}\right)\left(N_r\frac{\partial\xi_{ii}}{\partial N_k}\right) \tag{24}$$

$$\left(N_r\frac{\partial\eta}{\partial N_k}\right) = \frac{\varrho_r}{4}r_kb_k \tag{25}$$

$$\left(N_r\frac{\partial\xi_{ij}}{\partial N_k}\right) = \left(\frac{b_ib_j}{b_{ij}}\right)^{1/3}\frac{\varrho_r}{4}r_kb_k^{\ 2/3} \tag{26}$$

3. Critical Consolute Points

Critical consolute points in liquid mixtures satisfy the following equations which define a critical point for a m-component mixture:[31]

$$X = \begin{vmatrix} -P_\rho & P_{\phi_1} & \cdots & P_{\phi_{m-1}} \\ -P_{\phi_1} & A_{\phi_1\phi_1} & \cdots & A_{\phi_1\phi_{m-1}} \\ \vdots & \vdots & \ddots & \vdots \\ -P_{\phi_{m-1}} & P_{\phi_{m-1}\phi_1} & \cdots & A_{\phi_{m-1}\phi_{m-1}} \end{vmatrix} = 0 \tag{27}$$

$$Y = \begin{vmatrix} -X_\rho & X_{\phi_1} & \cdots & X_{\phi_{m-1}} \\ -P_{\phi_1} & A_{\phi_1\phi_1} & \cdots & A_{\phi_1\phi_{m-1}} \\ \vdots & \vdots & \ddots & \vdots \\ -P_{\phi_{m-1}} & P_{\phi_{m-1}\phi_1} & \cdots & A_{\phi_{m-1}\phi_{m-1}} \end{vmatrix} = 0 \tag{28}$$

where the elements of determinants X and Y are defined as

$$p_\varrho = \frac{1}{k_BT}\left(\frac{\partial p}{\partial\varrho_r}\right) \tag{29}$$

$$p_{\phi_l} = \frac{1}{\varrho_rk_BT}\left(\frac{\partial p}{\partial\phi_l}\right) \tag{30}$$

$$A_{\phi_l\phi_k} = \frac{\partial}{\partial\phi_k\partial\phi_l}\left(\frac{A}{N_rk_BT}\right) \tag{31}$$

$$X_\varrho = \varrho_r\frac{\partial X}{\partial\varrho_r} \tag{32}$$

$$X_{\phi_l} = \frac{\partial X}{\partial\phi_l} \tag{33}$$

The elements of determinants X and Y are expressed as dimensionless quantities.

For consistency, the polymer is always identified as the largest numbered component in the mixture and the solvent having the smallest value of r has the lowest number. For example, in a binary solvent/polymer mixture, the solvent is component 1 and the polymer is component 2. In a ternary mixture of two solvents and a polymer, the polymer is component 3 and the solvents are designated such that $r_1 < r_2$.

An attempt is made here to calculate critical solution temperatures that are consistent with those obtained from experimental cloud-point methods. In most cases, the vessel containing a solvent/polymer mixture also contains vapor space,[32,33] unless measurements are performed at an elevated pressure above the saturation pressure of the solution.[34-36] When phase separation occurs at temperatures approaching the critical temperature of the solvent (i.e., LCSTs), the vapor pressure above the solution can be significantly greater than 1 atm.

For consistency with experiment, calculations of critical consolute temperatures of binary mixtures are not at atmospheric pressure but at the vapor pressure of the solution. For mixtures considered here, the polymer is assumed nonvolatile and the vapor pressure of the mixture is determined by equating the chemical potentials of solvent in the liquid (L) to that in the vapor (V):

$$\mu_1^{\mathrm{L}}(\phi_1) = \mu_{\text{pure 1}}^{\mathrm{V}} \tag{34}$$

Therefore, calculation of the critical consolute point of a binary mixture involves four unknowns: the critical consolute temperature T_{CST} (upper or lower), the critical polymer segment fraction ϕ_{2c}, the segment density at the critical consolute point, and the vapor pressure of the mixture p^{sat}. These quantities are determined from four equations: the critical-point conditions eqs 27 and 28, the equation of state eq 6, and the equality of solvent chemical potential in the liquid to that in the vapor (eq 34).

Critical consolute points calculated assuming a fixed low pressure (zero or atmospheric) and those calculated as described above are necessarily different, but the difference is only significant for LCSTs. UCSTs in polymer solutions usually occur at temperatures near the triple-point temperature of the solvent where its vapor pressure is almost always much less than atmospheric.

4. Determination of Θ Conditions

To calculate Θ conditions using an equation of state for chainlike fluids, we consider the stability criterion of a binary mixture. Thermodynamic stability at some composition, temperature, and pressure can be determined by the sign of the second derivative of the Gibbs energy, G, with respect to the segment fraction of component 1, ϕ_1. If $(\partial^2G/\partial\phi_1^2)_{T,p} > 0$, the mixture is stable or metastable; otherwise, if $(\partial^2G/\partial\phi_1^2)_{T,p} < 0$, the mixture is unstable. Therefore, the relation $(\partial^2G/\partial\phi_1^2)_{T,p} = 0$ provides a convenient criterion for defining the limit of mixture stability.

To apply this criterion to determine the Θ temperature of a binary mixture, we make use of some important features of the Θ condition that evolve from the Shultz–Flory relation (eq 1). First, the Θ temperature is identical to the critical consolute temperature of a solution containing a polymer of infinite molecular weight. Second, the critical polymer segment fraction vanishes in this limit. Hence, a Θ temperature should correspond to a root of $(\partial^2G/\partial\phi_1^2)_{T,p}$ in the limit of infinite polymer molecular weight ($r_2 \to \infty$) and zero polymer segment fraction ($\phi_2 \to 0$). If in contact with its vapor, the pressure of the system is the vapor pressure of the pure solvent.

For a polymer (component m) mixed with $m - 1$ solvents, the appropriate criterion is:

$$\begin{vmatrix} G''(1,1) & \cdots & G''(1,m-1) \\ \vdots & \ddots & \vdots \\ G''(m-1,1) & \cdots & G''(m-1,m-1) \end{vmatrix} = 0 \qquad (35)$$

where

$$G''(i,j) \equiv \left(\frac{\partial^2 G}{\partial\phi_i\,\partial\phi_j}\right)_{T,p} \qquad (36)$$

The Θ temperature of a polymer in a fixed composition of $m - 1$ solvents is determined by the roots of eq 35 in the "Θ limit" (i.e., $r_m \to \infty$ and $\phi_m \to 0$).

However, evaluation of eq 35 is inconvenient because, when thermodynamic properties of a mixture are derived from a pressure-explicit equation of state, the derivatives of the Gibbs energy with respect to composition cannot be computed analytically. This problem is circumvented by variable transformations[31] which replaces the determinant in eq 35 with determinant X given by eq 27. Equation 27 expresses the stability criterion as derivatives of the Helmholtz energy and pressure with respect to segment density and composition that can be computed analytically. The two determinants are equivalent except for a difference in sign. In this work, Θ conditions are determined by finding the roots of determinant X in the Θ limit, denoted by X^∞. When $X^\infty > 0$, the mixture may phase separate at some concentration and polymer molecular weight. When $X^\infty < 0$, the polymer is miscible in all proportions with the solvent or solvent mixture, regardless of polymer molecular weight.

Determination of Θ temperatures for a binary mixture is illustrated in Figure 1 for a hypothetical solvent/polymer mixture where the solvent is composed of four spherical segments. The ratio of pure-component interaction energies and that for hard-core segment diameters are set equal to unity. For three binary interaction parameters κ_{12}, Figure 1 shows X^∞ as a function of temperature scaled by the critical temperature of the solvent. The pressure of the system is the vapor pressure of the pure solvent.

When $\kappa_{12} = 0$, the solvent is essentially a low-molecular-weight analog of the polymer. Because of compressibility differences which arise from size differences between solvent and polymer as temperature increases, a root of X^∞, corresponding to a "lower" Θ temperature Θ_L, occurs at a reduced temperature of approximately 0.76. A lower Θ temperature signifies that the mixture becomes unstable upon increasing temperature, as illustrated by the change in sign of X^∞ from negative below Θ_L to positive above Θ_L.

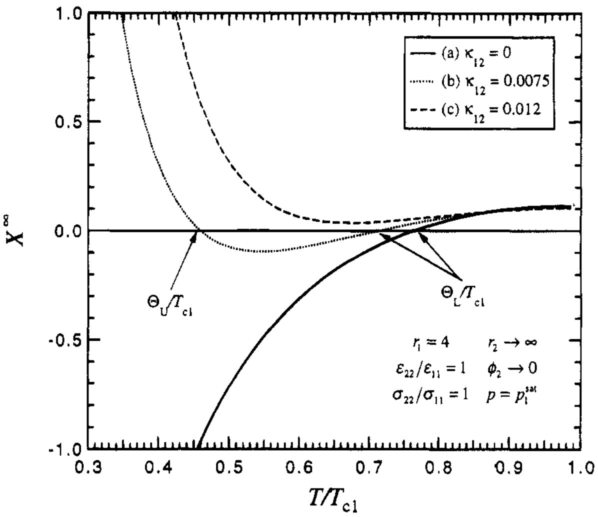

Figure 1. Calculation of Θ temperatures in a hypothetical solvent (1)/polymer (2) mixture. Θ temperatures are identified by roots of the spinodal criterion (eq 27), in the limit of infinite polymer molecular weight and zero polymer segment fraction.

A nonzero value of the binary interaction parameter introduces asymmetry in the pair interactions. When $\kappa_{12} = 0.0075$, a low-temperature root and a high-temperature root are observed. The high-temperature root corresponds again to Θ_L, whereas the low-temperature root corresponds to an upper theta temperature, Θ_U, and the change of sign of X^∞ indicates that the mixture becomes unstable upon decreasing temperature below Θ_U.

If the binary interaction parameter is increased further to $\kappa_{12} = 0.012$, X^∞ has a positive sign at all temperatures. Consequently, for some molecular weights and concentrations, the polymer is not completely miscible with the solvent at all temperatures. However, the low molecular weights of the polymer may be miscible at some conditions, as illustrated in Figure 2 which shows the Shultz–Flory plots (reciprocal critical solution temperatures vs $r^{-1/2} + (2r)^{-1}$ where $r = r_2/r_1$) corresponding to each value of κ_{12} used in Figure 1. In Figure 2c, the UCST and LCST merge as the molecular weight of the polymer increases, indicating hourglass-type phase diagrams in the temperature–composition plane. For the smaller values of κ_{12}, the intercepts on the vertical axes of parts a and b of Figure 2 correspond to the reciprocal reduced Θ temperatures identified from roots of X^∞ in Figure 1. Finally, the nonlinear behavior of the Shultz–Flory plots commonly observed experimentally is predicted by using an equation-of-state description of the fluid mixture.

Shultz–Flory plots for estimating Θ temperatures also provide a convenient means for "mapping" regions of miscibility as a function of temperature and polymer molecular weight. Having established a method for the determination of Θ temperatures in binary systems, the next section discusses how Shultz–Flory plots for several binary systems can be quantitatively correlated by using experimental Θ temperatures to determine

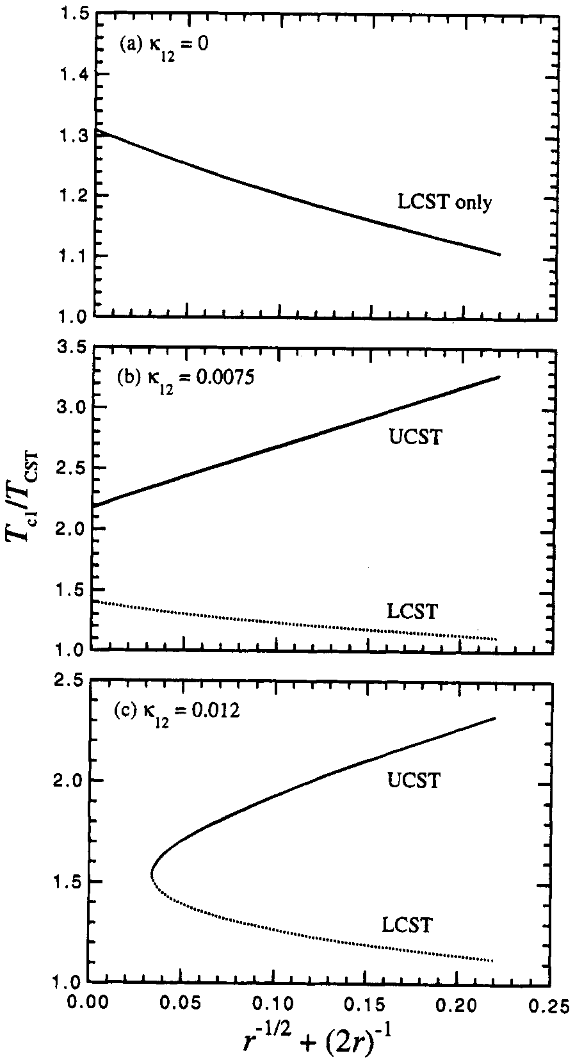

Figure 2. Shultz–Flory plots corresponding to the hypothetical solvent (1)/polymer (2) mixtures considered in Figure 1. (a) Only lower critical solution temperatures are observed; the vertical-axis intercept is T_{cl}/Θ_L. (b) Both upper and lower critical solution temperatures are observed; the intercepts on the vertical axis are T_{cl}/Θ_L and T_{cl}/Θ_U. (c) The upper and lower critical solution temperatures merge as polymer molecular weight increases, indicating hourglass-type phase diagrams; Θ temperatures do not exist for this system.

equation-of-state parameters. Parameters determined in this manner are then used to predict critical solution temperatures as a function of pressure, polymer molecular weight, and solvent composition.

5. Determination of Equation-of-State Parameters

Three parameters characterize each pure component in the mixture: the number of effective hard spheres per molecule r_i, the effective segment–segment interaction energy ϵ_{ii}, and the effective hard-core segment diameter, σ_{ii}. In addition, the PHSC equation of state also requires a binary interaction parameter κ_{ij} for each pair of components in the mixture. The number of effective hard spheres per molecule r_i for a polymer is linearly related to the polymer molecular weight; therefore, a polymer is more conveniently characterized by r_i/M_i, where M_i is the polymer molecular weight. However, when calculating Θ conditions, r_i (or r_i/M_i) is not required because the polymer molecular weight is infinite.

Table 2. PHSC Equation-of-State Parameters for Various Solvents

solvent	r	ϵ/k_B (K)	σ (Å)
n-pentane	3.149	226.0	3.995
n-hexane	3.446	235.6	4.084
n-heptane	4.255	225.9	3.947
n-octane	5.055	219.6	3.850
benzene	2.727	291.6	3.958
cyclopentane	2.509	277.3	4.090
cyclohexane	2.723	286.7	4.425
methylcyclohexane	2.968	283.7	4.336
methyl acetate	3.804	224.8	3.338
ethyl acetate	4.509	213.5	3.369
n-propyl acetate	4.989	213.9	3.440
isopropyl acetate	4.779	210.6	3.484
tert-butyl acetate	4.485	220.2	3.743

For a binary solvent/polymer mixture in the Θ limit, some thermodynamic properties of the mixture, for example, the vapor pressure and liquid density, reduce to the thermodynamic properties of the pure solvent, indicating the importance of characterizing the pure solvent. Therefore, equation-of-state parameters r_i, ϵ_{ii}, and σ_{ii} for solvents are determined by regression of vapor-pressure and saturated liquid-density data at temperatures between $0.5 < T/T_c < 0.9$, where T_c is the gas–liquid critical temperature of the solvent. Thermodynamic properties for all solvents considered here are obtained from the DIPPR pure-chemical-data compilation.[37] Table 2 gives the PHSC equation-of-state parameters for solvents considered here. The root-mean-square relative deviation between calculated and experimental vapor pressures and saturated liquid densities is 1–6%.

For quantitative correlation of experimental liquid–liquid equilibria, determination of pure-component parameters for polymers is less obvious. A common source of pure-polymer parameters is regression of liquid polymer *PVT* data; however, when used in conjunction with solvent parameters, quantitative correlation of experimental liquid–liquid equilibrium data has been largely unsuccessful regardless of which equation of state is used.[24,38,39] Adjusting binary interaction parameter κ_{ij} or adding a second binary parameter [e.g., relaxing the additivity of hard-sphere diameter constraint (eq 12)] does not give the equation of state enough flexibility to correlate LLE. The conventional procedure for using equations of state to correlate LLE is not satisfactory because, when pure polymer *PVT* data are used, parameters characterizing the polymer repeat unit differ significantly from the parameters for the solvent analog (e.g., the energy parameter for polyethylene is significantly different from for large molecular weight normal alkanes).[19]

Because polymer parameters obtained from *PVT* data cannot correlate LLE, we determine polymer parameters using judiciously chosen experimental data. First, the polymer segment diameter is set equal to that of the solvent, $\sigma_{22} = \sigma_{11}$. Second, for systems which only exhibit LCST behavior, the polymer–polymer segment interaction energy, ϵ_{22}, is adjusted to match the experimentally determined lower Θ temperature, Θ_L, and the binary interaction parameter, κ_{12}, is set to zero. For systems which exhibit both UCST and LCST behavior, both ϵ_{22} and κ_{12} are adjusted to match Θ_U and Θ_L. Using the parameters determined from Θ conditions, r_2/M_2 is determined by matching the critical solution temperature for a specific polymer molecular weight. If the critical solution temperature for more than one polymer molecular weight is available, the lowest mo-

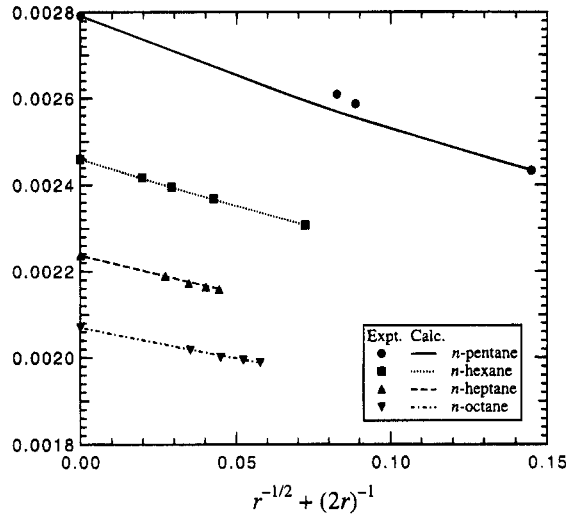

Figure 3. Shultz–Flory plots of lower critical solution temperatures of polyethylene in normal alkanes. The symbols on the vertical axis are the reciprocals of the reported Θ temperatures. Lines are calculated using the PHSC equation of state.

Table 3. PHSC Equation-of-State Parameters for Polyethylene (2) in Several Alkanes

solvent (1)	ϵ_{22}/k_B (K)	r_2/M_2 (mol/g)
n-pentane	225.5	0.03490
n-hexane	232.6	0.02026
n-heptane	222.9	0.02925
n-octane	216.2	0.02090

lecular weight is used and the critical solution temperatures at all other polymer molecular weights are predicted. If a system exhibits both UCST and LCST behavior, the UCST is chosen to determine r_2/M_2, and the LCSTs for systems with finite polymer molecular weights are predicted.

The decision to set the polymer and solvent segment diameters equal to one another was made for two reasons. First, it reduces by one the number of polymer parameters which must be determined from experimental data. Second, and perhaps more important, LLE for binary mixtures was better behaved in this limit. When all segment diameters were equal, the effects of the polymer–polymer interaction energy and the binary interaction parameter on Θ_U and Θ_L could be more easily anticipated and led to the proposed method for determining model parameters.

Abandoning the use of pure-polymer parameters which are independent of solvent may be unappealing from a theoretical statistical-mechanics standpoint, but we believe this drawback is outweighed by the increased flexibility and utility of the model. The increased flexibility results from allowing the pure-polymer parameters to take up some of the slack of representing binary mixture data that is typically reserved for additional binary parameters. The increased utility results from linking model parameters to *specific* experimental data which can be determined from one or more of the methods outlined in the Introduction.

6. Results and Discussion

The binary systems considered first are those showing only LCST behavior. Figure 3 shows the Shultz–Flory plots for polyethylene in normal alkanes (pentane through octane).[40] For each solvent, Table 3 gives the polyethylene interaction energy determined from the reported Θ_L. Also listed in Table 3 is the value of r_2/M_2 determined from the LCST of the lowest polyethylene molecular weight. For mixtures with pentane, the polyethylene molecular weight range studied was $M_w = 4.9 \times 10^3 - 14.3 \times 10^3$; for mixtures with hexane $M_w = 34.9 \times 10^3 - 4.421 \times 10^5$; and for mixtures with heptane and octane $M_w = 76.8 \times 10^3 - 2.02 \times 10^5$. The parameter estimation method used here fixes the two points at each end of the Shultz–Flory plot and predicts points in between. For systems with hexane, heptane, and octane, excellent agreement between calculated and experimental lower critical solution temperatures is observed. For systems with pentane, however, the LCSTs of the two higher polyethylene molecular weights are overestimated by approximately 5 °C. This discrepancy is due to uncertainty in the reported Θ_L since the polyethylene molecular weights used with pentane were much smaller than those used with the other solvents.

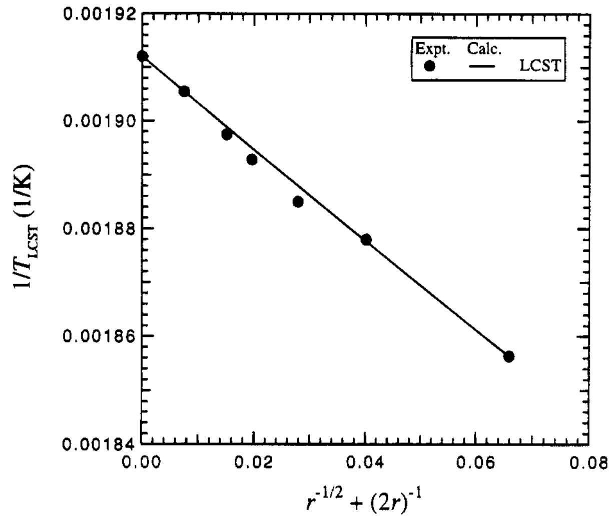

Figure 4. Shultz–Flory plots of lower critical solution temperatures of polystyrene in benzene. The line is calculated using the PHSC equation of state.

Table 4. PHSC Equation-of-State Parameters for Polystyrene (2) in Several Solvents

solvent (1)	ϵ_{22}/k_B (K)	κ_{12}	r_2/M_2 (mol/g)
benzene	237.3	0	0.01808
cyclopentane	245.0	0.01450	0.02112
cyclohexane	246.8	0.01458	0.03390
methylcyclohexane	253.7	0.01582	0.01877
methyl acetate	220.1	0.01192	0.01760
ethyl acetate	213.0	0.00678	0.03685
n-propyl acetate	212.5	0.00513	0.07100
isopropyl acetate	217.1	0.00567	0.02975
tert-butyl acetate	226.8	0.00678	0.01458

Similar results are shown in Figure 4 for polystyrene in benzene[7] which shows only LCST behavior. The equation-of-state parameters for polystyrene in benzene are listed in Table 4.

Shultz–Flory plots for polystyrene in various solvents which exhibit upper and lower critical solution temperatures have been widely studied; Table 4 gives pertinent parameters. The Shultz–Flory plot for polystyrene ($M_w = 43 \times 10^3 - 1.6 \times 10^6$) in cyclopentane[41,42] is shown in Figure 5. The polymer–polymer segment interaction energy ϵ_{22} and the binary interaction parameter κ_{12} were determined from the upper and lower Θ temperatures; r_2/M_2 was determined from the UCST reported for the lowest polystyrene molecular weight. Like the LCST Shultz–Flory plot for benzene, parameters are chosen to fix each end of the UCST Shultz–Flory plot. UCSTs in between are well correlated; the maximum error

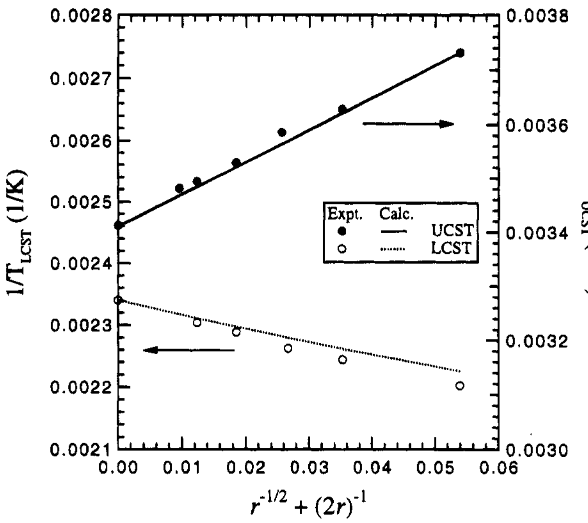

Figure 5. Shultz–Flory plot of lower (left axis) and upper (right axis) critical solution temperatures of cyclopentane/polystyrene solutions. Lines are calculated using the PHSC equation of state.

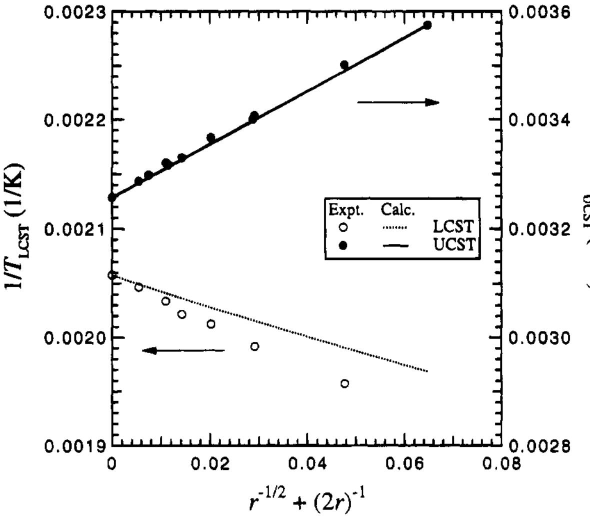

Figure 6. Shultz–Flory plot of lower (left axis) and upper (right axis) critical solution temperatures of cyclohexane/polystyrene solutions. Lines are calculated using the PHSC equation of state.

between calculated and experimental UCST is less than 1.7 °C. However, the lower critical solution temperatures for all finite polystyrene molecular weights are always underpredicted. The error between predicted and calculated LCSTs is 1.3 °C for the largest molecular weight and increases to 4.7 °C for the smallest molecular weight.

Similar results are obtained for polystyrene (M_w = 20.4 × 10^3–2.7 × 10^6) in cyclohexane[6,32] shown in Figure 6 and polystyrene (M_w = 10.2 × 10^3–2.7 × 10^6) in methylcyclohexane[6,43,44] shown in Figure 7. For both solvents the UCSTs are slightly overpredicted by at most 2 °C, and the LCSTs are underpredicted. For cyclohexane the maximum error between predicted and experimental LCSTs is 8.4 °C, whereas for methylcyclohexane the maximum difference is 5.6 °C.

The same behavior is also shown in Figures 8–11 for polystyrene (M_w = 37 × 10^3–2.7 × 10^6) in *n*-propyl acetate, isopropyl acetate, ethyl acetate, and methyl acetate[45] and in Figure 12 for polystyrene (M_w = 1 × 10^5–3.45 × 10^6) in *tert*-butyl acetate.[32,35] Except for *tert*-butyl acetate, UCSTs are correlated to within 1.5 °C. LCSTs are underpredicted more severely; the maximum errors between calculated and experimental LCSTs are 14.6, 11.2, 10.6, 8.1, and 8 °C, respectively, for *n*-propyl acetate, isopropyl acetate, ethyl acetate, methyl acetate, and *tert*-butyl acetate.

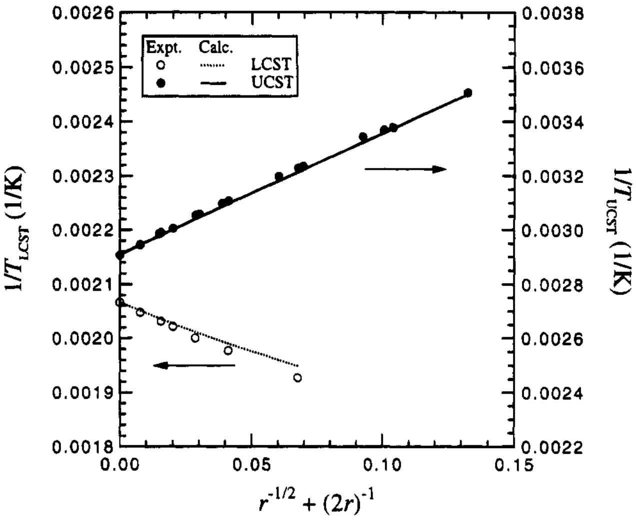

Figure 7. Shultz–Flory plot of lower (left axis) and upper (right axis) critical solution temperatures of methylcyclohexane/polystyrene solutions. Lines are calculated using the PHSC equation of state.

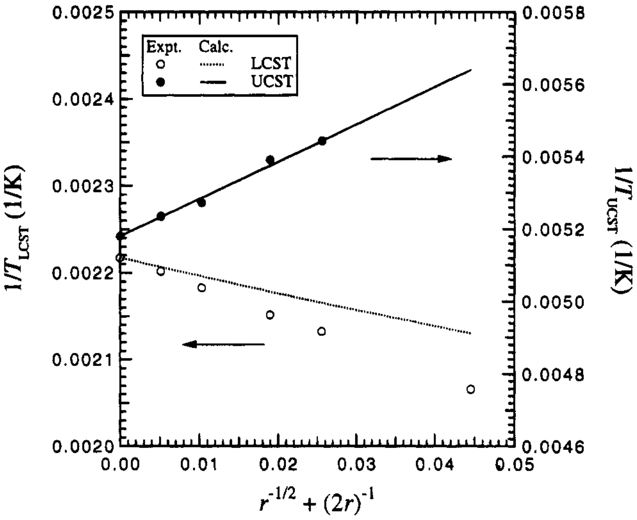

Figure 8. Shultz–Flory plot of lower (left axis) and upper (right axis) critical solution temperatures of *n*-propyl acetate/polystyrene solutions. Lines are calculated using the PHSC equation of state.

For *tert*-butyl acetate, data for the lowest polystyrene molecular weight from Saeki et al.[35] were used to determine r_2/M_2, since there appears to be some inconsistency between their results and the results of Bae et al.[32] for the molecular weight dependence of the UCST. The UCSTs from Bae et al.[32] are underpredicted by 9–12 °C. The PHSC equation of state predicts nonlinear curves for both the UCST and LCST in good agreement with experiment.

For *tert*-butyl acetate/polystyrene mixtures, data for Shultz–Flory plots at elevated pressures have also been measured. These data allow calculation of the effect of pressure on the upper and lower Θ temperature.[35] Using equation-of-state parameters determined from the Shultz–Flory plot at low pressure (Figure 12), Figure 13 shows excellent agreement between predicted and experimental upper and lower Θ temperatures for pressures up to 50 atm.

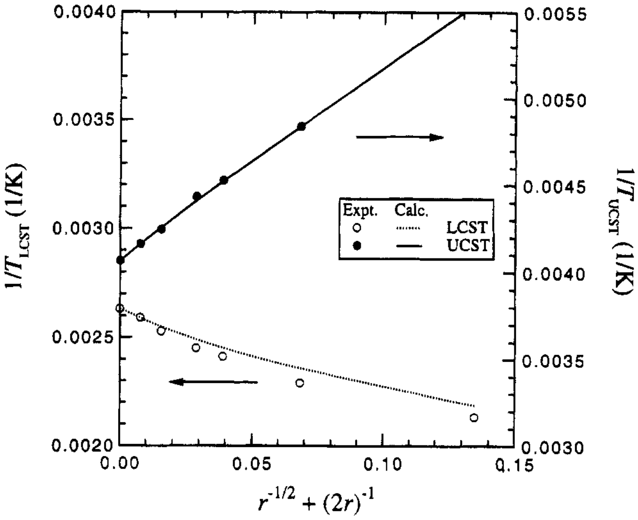

Figure 9. Shultz–Flory plot of lower (left axis) and upper (right axis) critical solution temperatures of isopropyl acetate/polystyrene solutions. Lines are calculated using the PHSC equation of state.

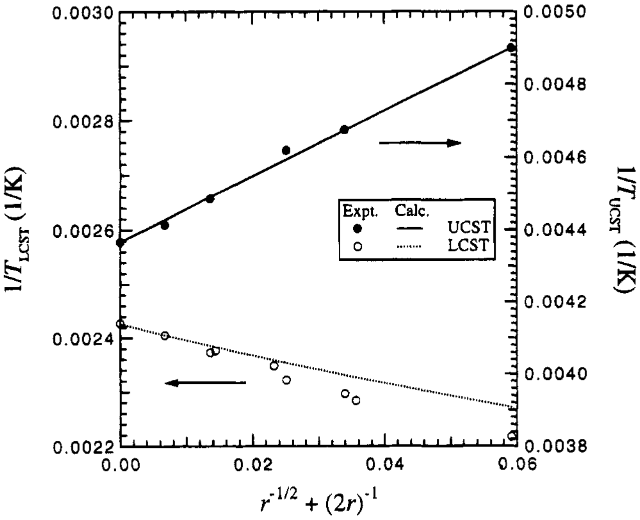

Figure 10. Shultz–Flory plot of lower (left axis) and upper (right axis) critical solution temperatures of ethyl acetate/polystyrene solutions. Lines are calculated using the PHSC equation of state.

Finally, we consider the upper Θ temperature of polystyrene in a mixed solvent containing cyclohexane and methylcyclohexane.[46] Because only the upper Θ temperature for the solvent mixture at low pressure is considered, calculations are performed assuming zero pressure. Also, polystyrene parameters must be determined. Noting that polymer parameters for each of the corresponding binary mixtures are similar, the polystyrene segment–segment interaction energy and hard-core segment diameter, ϵ_{33} and σ_{33}, are set to the average of the parameters for two solvents. The two solvent–polymer binary interaction parameters, κ_{13} and κ_{23}, are readjusted to match each binary upper Θ temperature, since ϵ_{33} and σ_{33} have been changed slightly. These parameters are listed in Table 5. Solvents which do not have comparable values of ϵ and σ may require a more severe adjustment of the solvent–polymer binary interaction parameters or an altogether different method for estimating "average" polymer parameters. The key step in any method, including the one used here, is matching the Θ temperatures for a polymer in each pure solvent. An approximate value for the solvent–solvent binary interaction parameter, κ_{12}, was obtained from analyzing vapor–liquid equilibrium data.[47] It was found that κ_{12} values ranging from 0 to 0.0035 give a nearly identical and quantitative representation of binary VLE data.

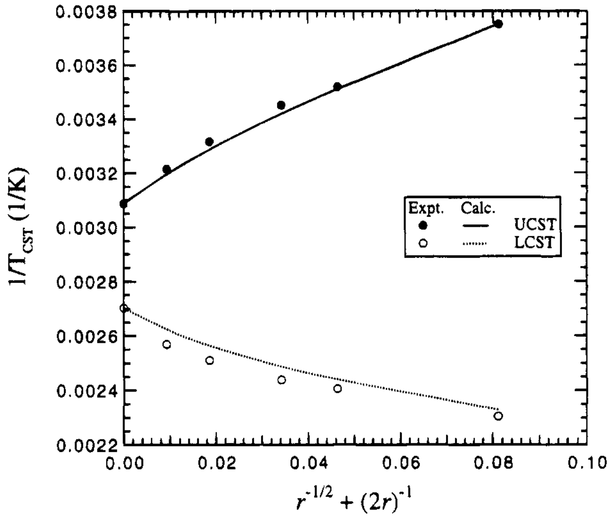

Figure 11. Shultz–Flory plot of lower and upper critical solution temperatures of methyl acetate/polystyrene solutions. Lines are calculated using the PHSC equation of state.

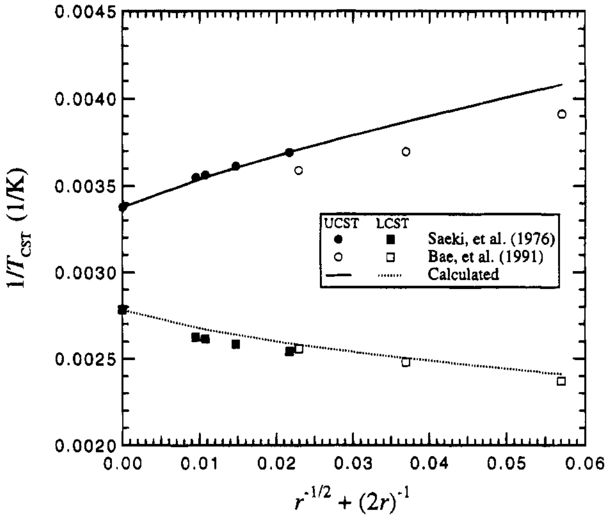

Figure 12. Shultz–Flory plot of lower and upper critical solution temperatures of *tert*-butyl acetate/polystyrene solutions. Lines are calculated using the PHSC equation of state.

Figure 14 examines the effect of the solvent–solvent binary interaction parameter, κ_{12}, on the upper Θ temperature. Experimentally determined upper Θ temperatures lie between the calculated curves which span the range of κ_{12} values estimated from solvent–solvent VLE data. Also shown is the curve for the value of κ_{12} which provides a quantitative correlation of the dependence of Θ_U on solvent composition. The curve for $\kappa_{12} = 0.01$ is included in Figure 14 to illustrate that the equation of state can predict a situation where Θ_U for the mixture is lower than that for either single-solvent system. In that event the polymer has an increased range of miscibility with the mixed solvent relative to that with either single solvent. It appears from this calculation that the polymer Θ temperature in a mixed solvent is much more sensitive than solvent–solvent VLE to small changes in the solvent–solvent binary interaction parameter. Consequently, using VLE data to obtain solvent–solvent binary interaction parameters may not necessarily lead to good predictions of the

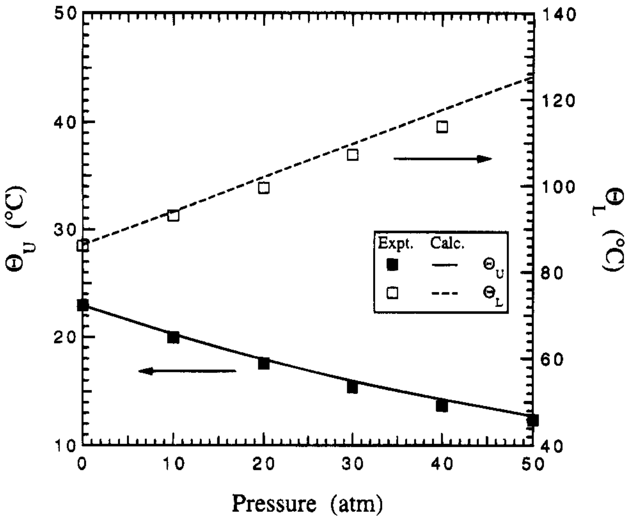

Figure 13. Pressure dependence of the upper (left axis) and lower (right axis) Θ temperatures for *tert*-butyl acetate/polystyrene solutions. The lines are predictions using the PHSC equation of state.

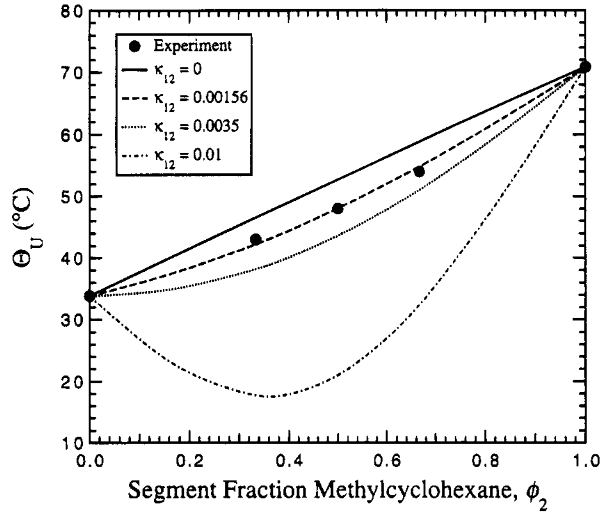

Figure 14. Dependence of upper Θ temperature on solvent composition for a ternary mixture of cyclohexane (1), methylcyclohexane (2), and polystyrene (3). Solvent–polymer binary interaction parameters (κ_{13} and κ_{23}) were chosen to match Θ_U for each binary. The solid curve and dotted curve represent the range of κ_{12} values which give a good representation of VLE for the solvent mixture (without polymer). The dashed curve represents the value of κ_{12} which best represents the solvent composition dependence of Θ_U. The dot-dashed curve represents a hypothetical system where Θ_U of the polymer in a mixed solvent is lower than that for either of the single-solvent/polymer systems.

Table 5. PHSC Equation-of-State Parameters for Polystyrene (3) Used To Calculate Upper Θ Temperatures in a Mixed Solvent of Cyclohexane (1) and Methylcyclohexane (2)

ϵ_{33}/k_B (K)	250.3
σ_{33} (Å)	4.396
κ_{13}	0.01658
κ_{23}	0.01424

polymer LLE. However, if used with caution, solvent–solvent VLE data could potentially be useful for screening polymer miscibility in mixed solvents.

7. Conclusion

By considering the thermodynamic stability criterion of mixtures, a method has been proposed for calculating Θ conditions using a perturbed hard-sphere-chain equation of state. This method uses two important results concerning the Θ condition which emerge from the Flory–Huggins model of incompressible mixture: (1) the Θ temperature is identical to the critical consolute temperature of a solution containing a polymer of infinite molecular weight and (2) the critical polymer segment fraction asymptotically approaches zero in the limit of infinite polymer molecular weight.

Θ temperatures, in conjunction with thermodynamic data for pure solvents and the critical consolute temperature of one polymer molecular weight, are used to determine equation-of-state parameters for binary mixtures. Parameters obtained in this manner provide a quantitative correlation of upper and lower critical solution temperatures as a function of polymer molecular weight and the upper and lower Θ temperatures at elevated pressures. Also, the Θ temperature of a polymer in a mixed solvent can be estimated from binary data. Although only one solvent mixture is considered here, we speculate that VLE data could be used to help screen solvent mixtures for desired polymer miscibility characteristics.

Although the method discussed here for determining equation-of-state parameters has the unfortunate consequence of making polymer parameters solvent dependent, it is important to note that the binary data chosen to determine equation-of-state parameters could be obtained even when only one polymer sample is available (albeit, monodisperse and of sufficiently large molecular weight). Θ temperatures (upper and lower), measured using a variety of methods, can be used to estimate two of the three equation-of-state parameters for the polymer. A single critical solution temperature, measured from cloud-point measurements, can be used to estimate the remaining polymer parameter.

Finally, we point out some limitations of the current model. First, the version of the PHSC equation of state used here cannot describe systems possessing specific or oriented interactions such as hydrogen bonding. For mixed solvent systems, self-associating solvents (such as alcohols) are often used as precipitating agents for fractionation, where knowledge of Θ conditions is very useful. For this reason, the majority of experimental data for Θ conditions of polymers in mixed solvents usually contain one self-associating solvent. However, the PHSC equation of state can be extended to include hydrogen-bonding components using the method of Veytsman.[48,49] Second, the PHSC equation of state used here is applicable only to solvent–homopolymer mixtures, but extension to copolymer and solvent–copolymer mixtures is straightforward.[21,50,51] For solvent–copolymer systems, the dependence of Θ conditions on copolymer composition can be obtained by extending the framework presented here.

Acknowledgment. This work was supported by the Director, Office of Energy Research, Office of Basic Energy Sciences, Chemical Sciences Division of the U.S. Department of Energy, under Contract No. DE-AC03-76SF00098. The authors are grateful to D. T. Wu (E. I. duPont de Nemours & Co., Philadelphia, PA) and R. Reijnhart (Koninklijke Shell Laboratories, Amsterdam, The Netherlands) for providing additional funding.

References and Notes

(1) Flory, P. J. *Principles of Polymer Chemistry*; Cornell University Press: Ithaca, NY, 1953.

(2) de Gennes, P.-G. *Scaling Concepts in Polymer Physics*; Cornell University Press: Ithaca, NY, 1979.

(3) Doi, M.; Edwards, S. F. *The Theory of Polymer Dynamics*; Oxford University Press: New York, 1986.

(4) Napper, D. H. *Polymeric Stabilization of Colloidal Dispersions*; Academic Press, Inc.: London, 1983.

(5) Shultz, A. R.; Flory, P. J. *J. Am. Chem. Soc.* **1952**, *74*, 4760–4767.

(6) Saeki, S.; Kuwahara, N.; Konno, S.; Kaneko, M. *Macromolecules* **1973**, *6*, 246–250.

(7) Saeki, S.; Kuwahara, N.; Konno, S.; Kaneko, M. *Macromolecules* **1973**, *6*, 589–593.

(8) Konno, S.; Saeki, S.; Kuwahara, N.; Nakata, M.; Kaneko, M. *Macromolecules* **1975**, *8*, 799–804.

(9) Elias, H.-G. *Makromol. Chem.* **1959**, *33*, 140–165.

(10) Elias, H.-G. *Makromol. Chem.* **1961**, *50*, 1–19.

(11) Elias, H.-G. In *Fractionation of Synthetic Polymers: Principles and Practices*; Tung, L. H., Ed.; Marcel Dekker, Inc.: New York, 1977.

(12) Napper, D. H. *Makromol. Chem.* **1968**, *120*, 231–234.

(13) Cornet, C. F.; van Ballegooijen, H. *Polymer* **1966**, *7*, 293–301.

(14) Talamini, G.; Bidotto, G. *Makromol. Chem.* **1967**, *110*, 111–122.

(15) Napper, D. R. *Polymer* **1969**, *10*, 181–185.

(16) Huglin, M. B. *Light Scattering from Polymer Solutions*; Academic Press: New York, 1972.

(17) Brandrup, J.; Immergut, E. H. *Polymer Handbook*, 3rd ed.; Wiley: New York, 1989.

(18) Sheng, Y.-J.; Panagiotopoulos, A. Z.; Kumar, S. K.; Szleifer, I. *Macromolecules* **1994**, *27*, 400–406.

(19) Song, Y.; Lambert, S. M.; Prausnitz, J. M. *Ind. Eng. Chem. Res.* **1994**, *33*, 1047–1057.

(20) Huang, S. H.; Radosz, M. *Ind. Eng. Chem. Res.* **1990**, *29*, 2284–2294.

(21) Song, Y.; Lambert, S. M.; Prausnitz, J. M. *Macromolecules* **1994**, *27*, 441–448.

(22) Song, Y.; Lambert, S. M.; Prausnitz, J. M. *Chem. Eng. Sci.* **1994**, *49*, 2765–2775.

(23) Sanchez, I. C.; Lacombe, R. H. *J. Phys. Chem.* **1976**, *80*, 2568–2580.

(24) Sanchez, I. C.; Lacombe, R. H. *Macromolecules* **1978**, *11*, 1145–1156.

(25) Panayiotou, C.; Vera, J. H. *Polym. J.* **1982**, *14*, 681–694.

(26) Panayiotou, C. G. *Macromolecules* **1987**, *20*, 861–871.

(27) Huang, S. H.; Radosz, M. *Ind. Eng. Chem. Res.* **1991**, *30*, 1994–2005.

(28) Boublik, T. *J. Chem. Phys.* **1970**, *53*, 471–472.

(29) Mansoori, G. A.; Carnahan, N. F.; Starling, K. E.; Leland, T. W. *J. Chem. Phys.* **1971**, *54*, 1523–1525.

(30) Prausnitz, J. M.; Lichtenthaler, R. N.; Azevedo, E. G. d. *Molecular Thermodynamics of Fluid Phase Equilibria*, second ed.; Prentice-Hall Inc.: Englewood Cliffs, NJ, 1986.

(31) Sadus, R. J. *High Pressure Phase Behavior of Multicomponent Fluid Mixtures*; Elsevier Science Publishers B.V.: Amsterdam, The Netherlands, 1992.

(32) Bae, Y. C.; Lambert, S. M.; Soane, D. S.; Prausnitz, J. M. *Macromolecules* **1991**, *24*, 4403–4407.

(33) Pfohl, O.; Hino, T.; Prausnitz, J. M. *Polymer*, in press.

(34) Saeki, S.; Kuwahara, N.; Nakata, M.; Kaneko, M. *Polymer* **1975**, *16*, 445–449.

(35) Saeki, S.; Kuwahara, N.; Kaneko, M. *Macromolecules* **1976**, *9*, 101–106.

(36) Saeki, S.; Kuwahara, N.; Hamano, K.; Kenmochi, Y.; Yamaguchi, T. *Macromolecules* **1986**, *19*, 2353–2356.

(37) Daubert, T. E.; Danner, R. P. *Physical and Thermodynamic Properties of Pure Chemicals. Data Compilation*; Hemisphere Publishing Corp.: New York, 1989.

(38) Kontogeorgis, G. M.; Fredenslund, A.; Tassios, D. P. *Ind. Eng. Chem. Res.* **1993**, *32*, 362–372.

(39) Kontogeorgis, G. M.; Harismiadis, V. I.; Fredenslund, A.; Tassios, D. P. *Fluid Phase Equil.* **1994**, *96*, 65–92.

(40) Hamada, F.; Fujisawa, K.; Nakajima, A. *Polym. J.* **1973**, *4*, 316–322.

(41) Iwai, Y.; Matsuyama, S.; Shigematsu, Y.; Arai, Y.; Tamura, K.; Shiojima, T. *Sekiyu Gakkaishi* **1990**, *33*, 117–121.

(42) Iwai, Y.; Shigematsu, Y.; Furuya, T.; Fukuda, H.; Arai, Y. *Polym. Eng. Sci.* **1993**, *33*, 480–485.

(43) Dobashi, T.; Nakata, M.; Kaneko, M. *J. Chem. Phys.* **1980**, *72*, 6685–6691.

(44) Dobashi, T.; Nakata, M.; Kaneko, M. *J. Chem. Phys.* **1984**, *80*, 948–953.

(45) Saeki, S.; Konno, S.; Kuwahara, N.; Nakata, M.; Kaneko, M. *Macromolecules* **1974**, *7*, 521–526.

(46) Abe, M.; Fujita, H. *J. Phys. Chem.* **1965**, *69*, 3263–3267.

(47) Ott, J. B.; Marsh, K. N.; Stokes, R. H. *J. Chem. Thermodyn.* **1980**, *12*, 1139–1148.

(48) Veytsman, B. A. *J. Phys. Chem.* **1990**, *94*, 8499–8500.

(49) Panayiotou, C.; Sanchez, I. C. *J. Phys. Chem.* **1991**, *95*, 10090–10097.

(50) Hino, T.; Song, Y.; Prausnitz, J. M. *Macromolecules* **1994**, *27*, 5681–5690.

(51) Hino, T.; Song, Y.; Prausnitz, J. M. *Macromolecules* **1995**, submitted.

MA946511L